Kerr-induced spontaneous Bessel beam formation in the regime of strong two-photon absorption

D. Faccio,[1,*] M. Clerici,[1] A. Averchi,[1] O. Jedrkiewicz,[1] S. Tzortzakis,[2] D. G. Papazoglou,[2,3] F. Bragheri,[4] L. Tartara,[4] A. Trita,[4] S. Henin,[4] I. Cristiani,[4] A. Couairon,[5] and P. Di Trapani[1,6]

[1]*CNISM and Dipartimento di Fisica e Matematica, Università dell'Insubria, Via Valleggio 11, Como, 22100, Italy*

[2]*Institute of Electronic Structure and Laser, Foundation for Research and Technology–Hellas (IESL-FORTH), P.O. Box 1527, 71110, Heraklion, Greece*

[3] *Materials Science and Technology Department, University of Crete, P.O. Box 2208, 71003, Heraklion, Greece*

[4]*Dipartimento di Elettronica, Università di Pavia, Via Ferrata 1, Pavia, 27100, Italy*

[5]*Centre de Physique Théorique, CNRS, cole Polytechnique, F-91128, Palaiseau, France*

[6]*Department of Quantum Electronics, Vilnius University, Sauletekio Avenue 9, 10222 Vilnius, Lithuania*

[*]*Corresponding author: daniele.faccio@uninsubria.it*

Abstract: We study the effect of Two-Photon Absorption (TPA) nonlinear losses on Gaussian pulses, with power that exceeds the critical power for self-focusing, propagating in bulk kerr media. Experiments performed in fused silica and silicon highlight a spontaneous reshaping of the input pulse into a pulsed Bessel beam. A filament is formed in which sub-diffractive propagation is sustained by the Bessel-nature of the pulse.

References and links

1. R. Boyd, *Nonlinear Optics* (Academic Press, 1992).
2. G. G. Luther, J. V. Moloney, and A. C. Newell, "Self-focusing threshold in normally dispersive media," Opt. Lett. **19**, 862–864 (1994)
3. A. Couairon, "Dynamics of femtosecond filamentation from saturation of self-focusing laser pulses," Phys. Rev. A **68**, 015801 (2003)
4. L. W. Liou, X. D. Cao, C. J. McKinstrie, and G. P. Agrawal, "Spatiotemporal instabilities in dispersive nonlinear media," Phys. Rev. A **46**, 4202–4208 (1992).
5. A. Couairon and A. Mysyrowicz, "Femtosecond filamentation in transparent media," Phys. Rep. **441**, 47–189 (2007).
6. M. Kolesik, E. Wright, and J. Moloney, "Dynamic nonlinear X waves for femtosecond pulse propagation in water," Phys. Rev. Lett. **92**, 253901 (2004).
7. D. Faccio, A. Averchi, A. Couairon, M. Kolesik, J. V. Moloney, A. Dubietis, G. Tamosauskas, P. Polesana, A. Piskarskas, and P. Di Trapani, "Spatio-temporal reshaping and X Wave dynamics in optical filaments," Opt. Express **15**, 13077–13095 (2007)
8. D. Faccio, A. Averchi, A. Lotti, P. Di Trapani, A. Couairon, D. Papazoglou, and S. Tzortzakis, "Ultrashort laser pulse filamentation from spontaneous X Wave formation in air," Opt. Express **16**, 1565–1570 (2008)
9. D. Faccio, A. Matijosius, A. Dubietis, R. Piskarkas, A. Varanavicius, E. Gaizauskas, A. Piskarkas, A. Couairon and P. Di Trapani, "Near and Far-Field evolution of laser pulse filaments in Kerr media," Phys. Rev. E **72**, 037601 (2005)
10. S. Tzortzakis, D. G. Papazoglou, and I. Zergioti, "Long-range filamentary propagation of subpicosecond ultraviolet laser pulses in fused silica," Opt. Lett. **31**, 796–798 (2006).

11. D. G. Papazoglou, I. Zergioti, and S. Tzortzakis, "Plasma strings from ultraviolet laser filaments drive permanent structural modifications in fused silica," Opt. Lett. **32**, 2055–2057 (2007).
12. R. Alfano, *Supercontinuum Laser Source* (Springer, 2005).
13. Q. Lin, O. J. Painter, and G. P. Agrawal, "Nonlinear optical phenomena in silicon waveguides: Modeling and applications," Opt. Express **15**, 16604–16644 (2007).
14. P. Polesana, A. Couairon, D. Faccio, A. Parola, M. A. Porras, A. Dubietis, A. Piskarskas, and P. Di Trapani, "Observation of conical waves in focusing, dispersive, and dissipative Kerr media," Phys. Rev. Lett. **99**, 223902 (2007).
15. M. A. Porras, A. Parola, D. Faccio, A. Dubietis, and P.Di Trapani, "Nonlinear unbalanced Bessel beams: Stationary conical waves supported by nonlinear losses," Phys. Rev. Lett. **93**, 153902 (2004).
16. D. Faccio, M. Porras, A. Dubietis, F. Bragheri, A. Couairon, and P. Di Trapani, "Conical emission, pulse splitting, and x-wave parametric amplification in nonlinear dynamics of ultrashort light pulses," Phys. Rev. Lett. **96**, 193901 (2006).

It is well known that in a Kerr medium, when the input power P exceeds a critical power P_{crit} the pulse undergoes self-focusing [1] and for high enough powers will collapse [2]. The pulse collapse will eventually be arrested by further effects which depend on the specific medium, e.g. group velocity dispersion and Nonlinear Losses (NLL) in condensed media or plasma defocusing in gases [3]. The large peak intensities reached during this process lead to the excitation of instabilities [4] whose nature depend drastically on the medium parameters and geometry. In literature the case of input Gaussian pulses propagating in transparent Kerr media with central wavelength far away from the material absorption band-edge, such that the number of photons involved in the nonlinear absorption is $K \geq 3$, has been extensively studied (see [5] and references therein). The instability shows a strong space-time coupling and will develop in the form of an on-axis supercontinuum and a conical emission, i.e. angularly dispersed frequencies. In the near field this instability is associated with the formation of X Waves [6, 7, 8, 9] and of a sub-diffractive high-intensity peak, i.e. a filament [5].

Recent experiments, performed for the first time in the regime of Two Photon absorption (TPA), i.e. $K = 2$, demonstrated filament formation [10] and waveguide writing [11] in fused silica samples using tightly focused Gaussian UV laser pulses. Here we present new experimental and numerical studies that highlight how large TPA leads to a substantially novel filamentation regime. Contrary to the standard ($K \geq 3$) filamentation case, no significant temporal dynamics are observed and the input Gaussian pulse is spontaneously reshaped only along the spatial coordinate into a Bessel profile. In order to prove the generality of our findings, we performed experiments in two very different material systems, which have in common TPA at the respective laser pump wavelengths.

A first experiment was carried out using an 8 mm long Silicon bulk sample. The pump laser pulse at 1550 nm was delivered by a *Ti:Sapph* pumped optical parametric amplifier (Topas, Light Conversion Ltd., Vilnius, Lithuania), had a temporal width of 100 fs (FWHM) and was spatially filtered. The pulse was then focused by a $f = 100$ mm lens placed 97 mm before the input facet of the sample. A half wavelength plate and a polarizer were used to continuously tune the energy in a range from 50 μJ to less than 1 nJ. Both near-field and angularly resolved spectra were recorded with a 12 bit digital InGaAs CMOS camera (XEVA, XenICs, Leuven, Belgium). The near field at the output plane of the sample was measured with a 10.6 times magnifying, single lens imaging system. The angularly resolved spectra were measured using a commercial imaging spectrometer (Shamrock, Andor Technology).

Figure 1(a) shows the Gaussian-like beam profile recorded at the very low input energy of 1.5 nJ (linear regime). The beam profile recorded at a higher input energy, namely 70 nJ (P $\sim 24\ P_{\mathrm{crit}}$) is shown in Fig. 1(b). Comparison between Fig. 1(a) and Fig. 1(b) evidences the reshaping that the Gaussian pump pulse undergoes during propagation, with the formation of a central peak surrounded by weaker rings. Figure 1(c) shows the (Gaussian) spectrum in the linear regime and Fig. 1(d) shows the output spectrum corresponding to the near field profile

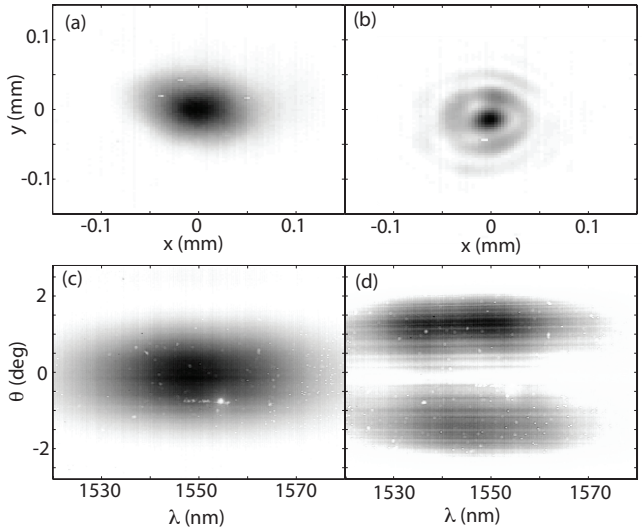

Fig. 1. Near field intensity profiles in (a) linear (1.5 nJ) and (b) nonlinear (70 nJ) regime respectively, of a 1550 nm, 100 fs pulse, after propagation in a 8 mm long Silicon bulk sample. (c) and (d) are the angularly resolved power spectra recorded for the same input conditions as (a) and (b), respectively.

in Fig. 1(b). A first observation is the surprising absence of any temporal spectral broadening. We recall once more that spectral broadening, and in particular supercontinuum generation are typical and expected phenomena at such large input powers (with respect to P_{crit}) [12]. On the other hand we notice a marked angular reshaping of the input pulse into a two peaked structure centered around $\theta = 0$, typical of a pulsed Bessel beam. We note that the first zero of the Bessel function $J_0(x)$ occurs at $x \sim 2.4048$ and that Bessel beams have an intensity profile defined by $I(r) = |J_0(k_\perp r)|^2$, where r is the radial coordinate and $k_\perp$ is the wave vector component perpendicular to the propagation direction. In accordance with this, the cone angle of the Bessel beam illustrated in Fig. 1(d) reveals that the corresponding pulsed Bessel beam should have the first zero in the near field radial profile for $r \sim 15\ \mu$m. This value is in agreement with the measured one of $\sim 16\ \mu$m (from Fig. 1(b)). In order to confirm the absence of temporal dynamics we performed a measurement of the temporal profile of the on-axis part of the pulse, in the conditions for which Fig. 1(b) and Fig. 1(d) were acquired. We measured the cross correlation between the pulsed Bessel beam and a 100 fs reference pulse @800 nm. The recorded trace (data not shown) is single-peaked and allows us to estimate that the reshaped pulse is also single peaked and has a temporal duration of 270 ± 15 fs. Linear dispersion ($k'' = 1.1 \times 10^4$ fs^2/cm) in silicon will broaden the input 100 fs pulse to 265 fs in 8 mm propagation, in close agreement with the measured value thus confirming that indeed no significant nonlinear temporal reshaping is taking place.

We point out that in Silicon other effects could play a relevant role in the reshaping process described in the present paper. In fact free carriers generated by TPA lead in turn to losses [13]. We note that no accumulation effects were observed as expected at our pulse repetition rate (KHz), due to the relatively short ($\sim \mu$s) free carrier recombination time. Furthermore, free carrier diffusion is negligible on the time scale of our 100 fs pulse. Thus, the overall effect of free carriers in bulk silicon may be viewed as an enhancement of the losses which will increase toward the trailing edge of the pulse. However the role of free carriers is not structural for the observed spatial reshaping as confirmed by the experiments performed in fused silica shown

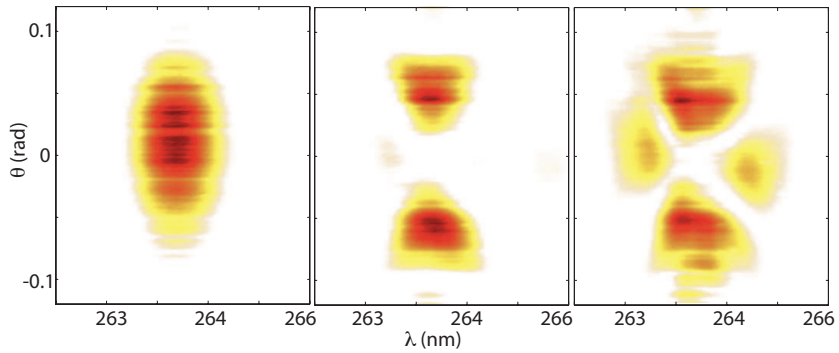

Fig. 2. Angularly resolved power spectrum (2 decade logarithmic scale) of a 264 nm, 200 fs pulse after propagation in a 13 mm long fused silica bulk sample for: (a) $P \ll P_{\text{crit}}$, (b) $P \sim 1.5\, P_{\text{crit}}$ and (c) $P \sim 3.5\, P_{\text{crit}}$.

below.

In order to highlight the generality of the spontaneous reshaping process shown here, we repeated the far field measurements in a very different TPA material system. To this end we characterized a sample of fused silica with a pump pulse of 200 fs (FWHM) time duration. The pump at 264 nm was obtained as the compressed fourth harmonic of a *Nd:glass* amplified laser system (Twinkle, Light Conversion Ltd., Vilnius, Lithuania). The pulse was spatially filtered and then focused by a f = 75 mm lens placed at 72 mm before the input facet of the 1 cm long fused silica sample. We recorded the angularly resolved power spectra with a 16 bit CCD camera (DU 420-OE, Andor Technology) combined with an imaging spectrometer (260-i, LOT-Oriel) and a f = 150 mm far-field lens. The results in the case of linear propagation (E = 15 nJ) and in the nonlinear regime (E = 110 nJ, P $\sim$ 1.5 P_{crit}) are shown in Fig. 2(a) and Fig. 2(b), respectively. It is clear from Fig. 2(b) that also in this case a spontaneous reshaping into a pulsed Bessel beam occurs. We were not able to directly measure the near field due to the extremely localized peak in combination with the high peak intensity and short UV wavelength. Finally in Fig. 2(c) we show the measured spectrum at a much higher input energy of 260 nJ (P $\sim$ 3.5 P_{crit}). The main Bessel peaks are still present along with distinct peaks on-axis at new wavelengths and weaker features that start to appear also at large angles close the central pump wavelength. These additional features are typical instabilities associated with intense Bessel beams as observed in Ref. [14] and show that simply increasing the input power will not lead to the usual filamentation dynamics observed with $K \geq 3$. Indeed for the case $K = 3$ a Gaussian input pulse reshaping was reported ([15]) in which a Bessel-like profile was experimentally observed, but only as a purely transient regime that then quickly evolved into a spatiotemporal X Wave [16]. On the other hand in this work the spontaneous evolution from the input Gaussian pulse into a pulsed Bessel beam is robust and increasing the input power leads to higher power propagating pulsed Bessel beams that may thus eventually develop Bessel-like instabilities. As a final comment we note that in both experiments the overall energy loss with respect to the input pulse was typically less than 30%.

We performed numerical simulations in the settings of the experiment in fused silica, i.e. with a 200 fs, 264 nm input Gaussian pulse that tightly focuses inside (z=0.4 cm) the 1 cm long sample. The numerics were performed using a model based on an extended Nonlinear Schrödinger equation described in detail elsewhere [5] with values of the nonlinear refractive index $n_2 = 2.6 \times 10^{-16}$ cm^2/W and of the nonlinear absorption coefficient $\beta_2 = 5.6 \times 10^{-11}$ cm/W. After the linear focus a pulsed Bessel beam emerges whose output spectrum, shown in

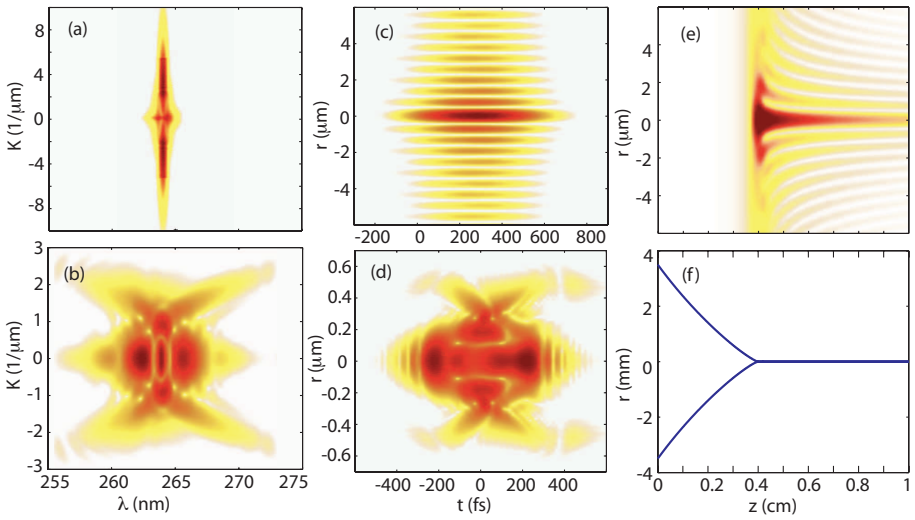

Fig. 3. Numerical simulations. (a) and (c) show the output pulsed Bessel beam spectrum and near-field profile in conditions that reproduce the experiments in fused silica. (e) and (f) show the fluence and radius at FWHM evolution along the propagation direction z. (b) and (d) show the results in exactly the same conditions as in (a) and (c) but with a nonlinear Kerr coefficient that is 5 times larger. All figures show the profiles over 3 decades in logarithmic scale.

Fig. 3(a), exhibits two distinct peaks at $\theta \sim \pm 0.07$ rad, in close agreement with the measured peaks at $\theta \sim \pm 0.06$ rad. The near-field distribution in Fig. 3(c) shows a clear spatial Bessel profile and no temporal modulations. Figure 3(e) shows the fluence profile around the central region (r$\sim$ 0) of the pulse: close to the linear focus at z=0.4 cm the pulse intensity increases sharply and a Bessel shaped pulse emerges that then propagates maintaining its profile notwithstanding some residual nonlinear losses that reduce the peak intensity. This may be also seen in Fig. 3(f) that shows the full-width at half maximum (FWHM) evolution of the pulse highlighting the initial linear focusing regime followed by the formation of a tight ($\sim 1\ \mu$m) sub-diffractive peak. In order to investigate the relative roles of TPA and Kerr nonlinearity, we repeated the same simulation after having artificially increased the Kerr nonlinearity by a factor 5. The results are shown in Figs. 3(b) and 5(d). In this case the initial evolution is dominated by a marked spatio-temporal focusing with the formation of an intense peak that is focused in both space and time. This leads to coupled spatio-temporal spectral instabilities, accompanied by pulse splitting and X Wave formation, typical of the usual filamentation regime. We note that nearly identical results were obtained by keeping n_2 fixed and reducing β_2. These findings clearly indicate that the suppression of the temporal instability and the spontaneous formation of a pulsed Bessel beam are related to a specific interplay between diffraction, the Kerr effect and TPA. Indeed we may define the respective characteristic lengths as $L_{\rm diff} = 2k_0w^2$, $L_{\rm kerr} = n_0/k_0n_2I$ and $L_{\rm tpa} = 2/\beta_2 I$, where w is the pulse half width at $1/e^2$, k_0 the pulse wave-vector and I is the peak intensity. Figure 4(a) shows the evolution of $L_{\rm diff}$ (solid line), $L_{\rm kerr}$ (long-dashed line) and $L_{\rm tpa}$ (short-dashed line) for the same simulation in Fig. 3(a), i.e. using parameters for fused silica, while for Figs. 4(b) and (c) the simulations have been repeated with n_2 increased by a factor 5 (with fixed β_2) and with β_2 decreases by a factor 5 (with fixed n_2), respectively. As may be seen, the spontaneous pulsed Bessel beam formation dynamics associated with Fig. 4(a) [and shown in detail in Figs. 3(a), (c), (e) and (f)]

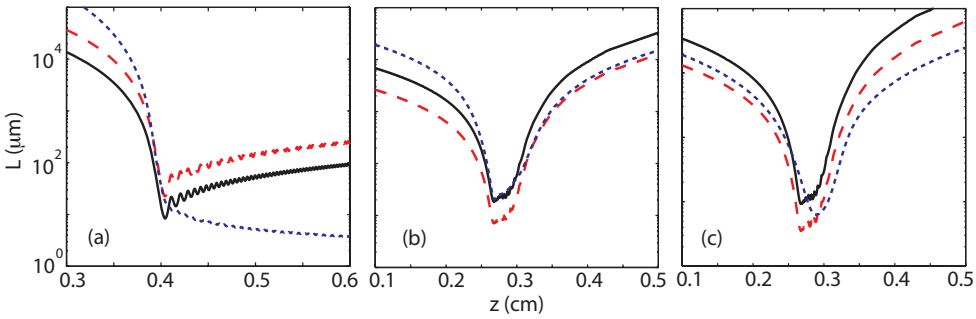

Fig. 4. Numerically evaluated evolution of $L_{\rm tpa}$, $L_{\rm diff}$ and $L_{\rm kerr}$. The simulations were performed using the same input pulse conditions of the experiment and (a) $n_2 = 2.6 \times 10^{-16}$ cm^2/W, $\beta_2 = 5.6 \times 10^{-11}$ cm/W, (b) $n_2 = 13 \times 10^{-16}$ cm^2/W, $\beta_2 = 5.6 \times 10^{-11}$ cm/W, (c) $n_2 = 2.6 \times 10^{-16}$ cm^2/W, $\beta_2 = 1.12 \times 10^{-11}$ cm/W.

are dominated before the focus by TPA, i.e. $L_{\rm tpa} < L_{\rm diff}, L_{\rm kerr}$. This indeed may be identified as the condition required for the observation of spontaneous pulsed Bessel beam formation. On the contrary, if the medium parameters are such that $L_{\rm tpa} > L_{\rm diff}$, the Kerr nonlinearity will lead to space-time focusing and the amplification of X-shaped spatiotemporal instabilities as shown in Figs. 3(b) and (d). We note that the given condition, $L_{\rm tpa} < L_{\rm diff}, L_{\rm kerr}$ (at every point before the beam focus), is peculiar of the TPA regime as $L_{\rm tpa}$ and $L_{\rm kerr}$ have the same dependence on the pulse intensity I.

Finally, the spontaneous reshaping of the Gaussian pulse into a Bessel pulse may be understood by noting that TPA acts as a distributed semi-opaque stopper placed in the center of the beam. In propagation a bright spot will form on axis, known as the Poisson or Arago spot and is described by a zero-order Bessel function. In other words the combined effects of the Kerr nonlinearity, TPA and diffraction lead to a reshaping into a conical pulse with the energy redirected around the edges of the stopper toward the center of the beam. In the presence of strong TPA this effect appears to occur only in the spatial dimension and in the temporal dimension no significant reshaping takes place. It is important to note that this will remain true only in the normal GVD regime. On the contrary, the anomalous GVD regime is formally analogous to the diffraction so that, under appropriate temporal focusing conditions, we may expect to observe a Bessel-like reshaping in both space and time.

In conclusion, we have shown that in the presence of strong TPA, a Gaussian pulse propagating in a Kerr medium with a power that exceeds the critical power for self-focusing, reshapes into a pulsed Bessel beam. Therefore, the conditions for a new regime of filamentation are reported, in which no temporal dynamics are observed and self-guiding is supported by the Bessel-nature of the pulse. Finally we speculate that, in analogy with Ref. [14], an appropriate excitation of the pulsed Bessel beam may even lead to the suppression, mediated by NLLs, of all temporal instabilities and of the related peak intensity fluctuations during the pulse propagation.

M.C. acknowledges the support from Sixth EU Framework Programme Contract No. MEST-CF-2004-008048 (ATLAS) and MIUR, project RBIN04NYLH. D.F. and P.D.T. acknowledge financial support from CNISM, INNESCO project. The research was partially funded by Italian Minstry of Research, PRIN05. ST acknowledges support from the Marie Curie Excellence Grant MULTIRAD MEXT-CT-2006-042683.